JOURNAL OF MATERIALS SCIENCE 28 (1993) 5963–5974

Review
Dislocation network models for recovery creep deformation

LONGQUAN SHI, D. O. NORTHWOOD
Engineering Materials Group, Mechanical Engineering Department, University of Windsor, Windsor, Ontario, Canada N9B 3P4

The development of dislocation network models for recovery creep and the important results which arise from the application of the models are discussed. These models are basically aimed at describing the two simultaneous processes, namely strain hardening and recovery, which occur during high-temperature creep deformation. These processes are modelled using detailed dislocation mechanisms which occur in the deforming crystalline materials. The present models, although still being approximations, are reasonably well able to describe high-temperature recovery creep deformation of crystalline materials.

1. Introduction

In dislocation creep, crystalline materials are classified into two categories (Class I and Class II) depending on their rate-controlling mechanism [1]. Pure metals and single-phase alloys in which creep is recovery-controlled (dislocation climb) are referred to as Class II materials, while Class I consists mainly of solid solutions in which the rate-determining process in creep is believed to be the viscous glide of solute-dragging dislocations [2]. Extensive research has been undertaken to understand the mechanisms of, and the transitions between, the two types of creep behaviour for a number of metals and solid solution alloys [3–12]. Recovery creep is believed to be an outcome of the interplay between the processes of strain-hardening and recovery. Bailey [13] postulated that steady-state creep represents the stage during which a dynamic balance is achieved between the strengthening effect of strain hardening and the softening induced by recovery. This basic concept was later formulated by Orowan [14] in the well-known Bailey–Orowan equation [13, 14]

$$\dot{\varepsilon} = \frac{R}{H} \tag{1}$$

where $\dot{\varepsilon}$ is the creep strain rate, $R = -(\partial\sigma/\partial t)$ is the rate of recovery, $H = (\partial\sigma/\partial\varepsilon)$ is the strain hardening coefficient, and σ is the applied stress. Numerous experiments have since been carried out by various investigators to check the validity of Equation 1 for recovery creep deformation [15–22]. Most of these experiments involve making a stress change to the creeping specimen and measuring the instantaneous strain generated (stress increment) or the incubation time (stress decrement) to obtain the strain-hardening coefficient, H, and the recovery rate, R, respectively.

The Bailey–Orowan recovery creep model has since been refined by, among others, Cottrell and Aytekin [15], McLean [23], Lagneborg [24], and Gittus [25]. As was pointed out by Lagneborg [26], the earlier recovery creep models did not describe the details of the deformation process [13, 14]. However, the more recent formulations, e.g. [23, 24], consider the mechanisms in some detail. In accord with direct experimental observations, these authors assume the dislocations to be arranged in a three-dimensional network during creep deformation. This "physical picture" is based on the early ideas of Frank [27] that the microstructure of a deformed single-phase crystalline solid consists of a three-dimensional array of dislocation segments arranged in the so-called Frank network. The creep process consists of consecutive events of recovery and strain hardening. The primary and steady-state creep processes are then described by the detailed movement of dislocation links within the three-dimensional network.

In this review, the development of network models and link length distribution models for recovery creep is discussed, within the context of two simultaneous processes, i.e. strain hardening and recovery, occurring within the three-dimensional dislocation network structure. It is interesting to note that this development of network models for recovery creep has taken place in parallel with experimental observations on the dislocation microstructure and a great number of empirical creep studies on the effects of temperature (activation energy), stress (stress exponent), and stacking fault energy on steady-state creep rate. It is shown that further work on subgrain formation and network coarsening kinetics is required in order to extend the present link length distribution models to their full potential.

2. Network models for recovery creep

Many direct observations have shown that the dislocation microstructure is in the form of

0022–2461

a three-dimensional network during recovery creep. Such a network structure has been found for example in pure α-iron crept at 823 K [28], copper–10 at % nickel alloy crept at 873 K [29], an austenitic stainless steel crept at 973 K [30], creep-deformed poly-crystalline MgO [31], monocrystalline aluminium and NaCl [32], and pure polycrystalline nickel [33], using both transmission electron microscopy and etch pit techniques. It was found that the link lengths in the dislocation network have a typical statistical distribution, and this information has been used to describe creep deformation process by link length distribution models. However, the early network models for recovery creep used only the average values (e.g. mobile dislocation density, the average space between dislocation links, etc.) because it was a practical and simple way to deal with the otherwise complicated recovery creep process.

2.1. McLean's model

McLean [34] has identified the recovery process as being the growth of the dislocation network, and utilizes Friedel's analysis of network growth [35]. The dislocation network coarsening kinetics as developed by Friedel [35], uses a similar analysis to that previously applied to grain growth. If $\langle\lambda\rangle$ is the mean mesh size of the three-dimensional network, the total length per unit volume of dislocation is $\rho = 1/\langle\lambda\rangle^2$, and the total dislocation energy per unit volume is therefore proportional to $1/\langle\lambda\rangle^2$, which gives the network an in-built tendency to coarsen. The driving force for such a dislocation network growth is inversely proportional to the average mesh size, or the average link length, $\langle\lambda\rangle$. That is

$$\frac{\mathrm{d}\langle\lambda\rangle}{\mathrm{d}t} \propto \frac{1}{\langle\lambda\rangle} \tag{2}$$

There is a theoretical justification for associating network growth with softening because the elastic force between dislocations is proportional to $1/\langle\lambda\rangle$, as given in the Orowan relationship [36, 37] for the flow stress, σ

$$\langle\lambda\rangle = \frac{\alpha\mu\boldsymbol{b}}{\sigma} \tag{3}$$

where α is a constant of the order of unity, μ is the shear modulus, and $\boldsymbol{b}$ is Burgers vector. From Equations 2 and 3 it follows that the recovery rate, $R = -(\partial\sigma/\partial t)$, is given by

$$R \propto \sigma^3 \tag{4}$$

This relationship, Equation 4, is supported by experimental creep data measured for nickel at 923–1023 K ($R \propto \sigma^3$) and aluminium at 473–523 K ($R \propto \sigma^{3.5}$) [17]. On the other hand, plastic deformation (strain-hardening [38, 39]) has an opposite effect to that of recovery and refines the three-dimensional network. Each moving dislocation will be held up in some location (e.g. locations where the network is fine) and bows between these points, so that its length increases. Occurring at many places, this kind of event has the effect of increasing the average dislocation density. In a polycrystalline metal undergoing plastic deformation, there is multiple slip in most, if not all, grains, and the refining action should be isotropic. The network need not therefore change its geometry greatly as the meshes become smaller. The refining action during which Equation 3 holds, is measured by the strain-hardening coefficient, H. Deformation at high temperatures can thus be described as the "struggle" of the three-dimensional network to accommodate the simultaneous refining and coarsening actions, corresponding to strain-hardening and recovery, respectively. In the equilibrium state, i.e.: steady-state creep, the average mesh size is fixed by Equation 3; the recovery rate, R, or coarsening of the network, is determined by Equation 4, and creep has to take place at the rate, $\dot{\varepsilon}$, which just offsets this coarsening. This balanced state is stable in the sense that an increase or decrease in average mesh size is automatically corrected [34]. This dynamic balance between strain hardening (mesh refining) and recovery (mesh coarsening) then is described by the Bailey–Orowan equation [13, 14].

McLean's recovery creep model [34] is important in that it began the network description of recovery creep deformation. Both strain hardening and recovery processes are now linked to the dislocation network microstructure and its dynamic movement for steady-state deformation at high temperature. A number of more accurate formulations for the recovery and strain-hardening processes were then initiated on the balanced state of the Bailey–Orowan equation for recovery creep.

2.2. Gittus's theoretical creep equation

Gittus [40] has developed a theoretical equation for steady-state dislocation creep. In obtaining this equation, the creeping material is assumed to contain a dislocation network in which a balance exists between the strain hardening due to dislocation generation and the recovery due to network recovery climb. The theoretical creep equation has the same form as the standard constitutive equation for steady-state creep [41–50]

$$\dot{\varepsilon}_s = A\frac{D_v\mu\boldsymbol{b}}{kT}\left(\frac{\sigma}{\mu}\right)^n \tag{5}$$

where A and the stress exponent, n, are dimensionless materials constants, D_v is the bulk self-diffusion coefficient, k is Boltzmann's constant, and T is the absolute temperature. Gittus's model [40] gives $A = 8\pi^3 C_j$ and $n = 3$, where C_j is the jog concentration. In developing Equation 5, it was assumed that the materials obey the Bailey–Orowan equation [13, 14], Taylor's strain-hardening model [51, 52], and Friedel's network-climb recovery equation [35]. The strain hardening coefficient, H, has been obtained by Evans [53] using a three-dimensional dislocation network model, which is

$$\frac{\partial\sigma}{\partial\varepsilon} = \frac{\mu}{2\pi} \tag{6}$$

The recovery rate, R, is obtained from Friedel's argument [35] that the rate at which a dislocation network will coarsen due to jog-controlled climb, is following essentially the same line as in McLean's model [34]. This results in

$$\frac{\partial \sigma}{\partial t} = -\frac{4D_v \boldsymbol{b} C_j \pi^2 \sigma^3}{\mu k T} \quad (7)$$

By substituting Equations 6 and 7 into the Bailey–Orowan Equation 1, one obtains the theoretical equation, namely [40]

$$\dot{\varepsilon}_s = (8\pi^3 C_j)\frac{D_v \mu \boldsymbol{b}}{kT}\left(\frac{\sigma}{\mu}\right)^3 \quad (8)$$

Comparison of experimental creep data has been made with that predicted by Equation 8 for nineteen crystalline metals, semi-conductors and ceramics. In several cases the predicted and actual creep strengths differ by less than a factor 2. The fit is poor in the case of germanium and MgO, and reasonably good for nickel, cadmium, β-thallium and stoichiometric UO_2 [40]. This recovery-hardening model of dislocation creep [40] has since been extended [54] to handle the solute-drag effect. This extended model considers the case where the dislocations are subject not only to the stress which the dislocation network imposes on each of its component segments, but also to a friction stress due to solute drag. It is shown that the solute-drag effect reduces the creep rate in Equation 8 by a factor $K = \{1 - [1 + kT/(A_0 2\pi D_v \boldsymbol{b} C_j)]^{-1}\}^3$, where $A_0 = \boldsymbol{b}F/v$ is a temperature-dependent constant whose exact value depends on the particular mechanisms by which the solute controls the dislocation motion, which is determined by the theoretical proportionality between friction stress, F, and dislocation velocity, v [54]. If there is no solute-drag friction stress ($F = 0$), then the factor $K = 1$ and Equation 8 applies to the case where solute-drag effect is zero.

2.3. Evans and Knowles' model

As has already been discussed, all of the recovery creep models are based on the assumption that the activation energy for creep, Q_c, is equal to that for lattice diffusion, Q_l. In fact, values of Q_c appreciably less than that for lattice diffusion, Q_l, are frequently found at typical creep test temperatures for a number of materials, such as aluminium [55], copper [56], tungsten [57], and thallium [58]. Also, the measured values of the stress exponent, n, are often significantly higher than those predicted by these theories: i.e. $n = 3$ [40] and $n = 4$ [59]. Evans and Knowles [60, 61] have developed a recovery creep model which accounts for the range of observed values in Q_c and n. Reasonable agreement has been found in comparing their model predictions with the experimental creep results for a range of materials including f c c metals (aluminium, copper, lead, nickel), b c c metals (α-iron, β-thallium), h c p metals (magnesium, zinc, cadmium), and non-metals (magnesium oxide, polycrystalline ice, stoichiometric uranium dioxide, polycrystalline alumina, lithium fluoride).

Evans and Knowles' model is based on a consideration of the rate-controlling process within a three-dimensional network and the vacancy flux through the lattice or along the dislocation core. Three components of the climb force considered in the model, these being: (i) the contribution of the applied stress, $\sigma \boldsymbol{b}/2$; (ii) the elastic interaction between links, $\mu \boldsymbol{b}^2/\{2\pi(1 - \nu)\langle\lambda\rangle\}$; and (iii) alterations in dislocation density, $\mu \boldsymbol{b}^2/\langle\lambda\rangle$. The overall climb force is taken as the sum of the above three forces. It is first shown that the climb of link dislocations is rate determining, because the climb velocity of the network nodes, v_n, is always faster than that of link dislocations, v_l. The ratio of climb velocities of node and link is given by

$$\frac{V_n}{V_l} = 2\ln\left(\frac{\langle\lambda\rangle}{2\boldsymbol{b}}\right) \quad (9)$$

This ratio is always larger than 1 and has typical values > 10. The above equation is arrived at via a diffusion path through the lattice. The same result holds if the dominant diffusion path is along the dislocation cores rather than through the lattice. It is assumed in the model [60, 61] that (i) creep strain arises entirely from the glide of edge dislocations from one pinning point in a three-dimensional network to another; this glide step occurs instantaneously; (ii) the slip distance, s, will be either the average network spacing, $\langle\lambda\rangle$, or a constant, independent of the network; (iii) the release of the arrested dislocations occurs either by rupture of a network node or by operation of a Frank–Read source from a network link; (iv) any value of link length between Burgers vector, $\boldsymbol{b}$, and the critical Frank–Read length is equally likely so that the approximate distribution of link lengths is rectangular; and (v) the climb rate contributions from lattice diffusion and pipe diffusion are likely to be independent of each other, similar to the case for the models where grain-boundary diffusion (Coble creep [62]) and lattice diffusion (Nabarro-Herring creep [63, 64]) are independent rate processes for a polycrystalline solid crept at high temperatures [47]. A general creep equation is then obtained by the summation of the respective contributions from lattice diffusion and pipe diffusion. The creep strain-rate equation is given by

$$\dot{\varepsilon} = A_e \frac{D_e \mu \boldsymbol{b}}{kT}\left(\frac{\sigma}{\mu}\right)^3 \quad (10)$$

for the case where the slip distance, s, of the released link is equal to the average spacing of the network $\langle\lambda\rangle$, i.e. $s = \langle\lambda\rangle$. The corresponding equation where s is a constant, which is independent of $\langle\lambda\rangle$, is given by

$$\dot{\varepsilon} = A_e \frac{D_e \mu s}{\alpha k T}\left(\frac{\sigma}{\mu}\right)^4 \quad (11)$$

where

$$A_e = \frac{4.2\,3^{1/2}\pi}{\alpha^2}\left\{1 + \frac{2}{\alpha}\left[1 + \frac{1}{2\pi(1 - \nu)}\right]\right\} \quad (12)$$

and

$$D_e = \left\{ \frac{D_l}{\ln[\alpha\mu/(2\sigma)]} + \frac{3D_p\sigma^2}{\alpha^2\mu^2} \right\} \quad (13)$$

and ν is Poisson's ratio.

The ratio of the terms on the right-hand side of Equation 13 reflects the diffusion path taken. This is given by

$$P = \frac{\alpha^2\mu^2 D_l}{3\sigma^2 D_p \ln[\alpha\mu/(2\sigma)]} \quad (14)$$

When $P \gg 1$, lattice diffusion predominates and $Q_c \approx Q_l$, whereas for $P \ll 1$, pipe diffusion prevails and $Q_c \approx Q_p$. The transition in diffusion path takes place when $P \approx 1$, and Equation 14 reduces to

$$\frac{D_l}{D_p} = \frac{b^2 \ln[\langle\lambda\rangle/(2b)]}{l^2} \quad (15)$$

for this special case. In Equations 9 to 15 $\langle\lambda\rangle = \alpha\mu b/\sigma$ is the average mesh size or the average distance between dislocation links, α is a constant of order unity, l is an individual link length, $D_l = D_0 C_0 \Omega$ is the lattice diffusion coefficient, D_0 is the vacancy diffusion coefficient, C_0 is the equilibrium vacancy concentration, Ω is the atomic volume, D_p is the pipe diffusion coefficient. If D_l/D_p is less than the right-hand side of Equation 15, then pipe diffusion will be the dominant transport process, which gives rise to a low value for Q_c. At high temperatures, the major diffusion path is through the lattice, whereas at lower temperatures, pipe diffusion along the network dislocation cores predominates. Also, a stress dependence of about 3 is predicted at high temperatures for $s = \langle\lambda\rangle$ and a value of 5 at lower temperatures. The corresponding values for s = constant are about 4 and 6, respectively.

It is interesting to note that the model equations, Equations 10 and 11, reduce to the form of the Dorn equation, Equation 5, when creep is controlled predominantly either by lattice diffusion or pipe diffusion, as is also the case for Gittus's model [40, 54]. The Dorn equation (Equation 5) is shown to have physical validity only for a stress dependence of 3 for lattice diffusion control or for a value of 5 for pipe diffusion control provided the appropriate diffusion coefficients are used [60, 61].

3. Link-length distribution models

In all the models discussed above, the dislocation network structure, which at the same time produces considerable hardening and provides mobile dislocations for glide, is either ignored entirely or at best described by an average quantity, the dislocation density, which in turn is related to the average link length. Although the evolutionary behaviour of the three-dimensional network is considered in some of the network models [18, 60, 61, 65–67], the general conclusions are drawn from the average characteristic values of the link-length distribution without going into details of how the distribution functions themselves evolve. This is clearly an oversimplification. In an actual material, dislocation links will always occur over a whole spectrum of lengths [26]. In the following sections, the models based on the link-length distribution, which derive creep strain rate and other quantities from the detailed movement of the three-dimensional network, will be discussed.

3.1. Öström and Lagneborg's link-length distribution model

Lagneborg and his associates [68–71] appear to be the first to have examined the details of link-length distribution from a physical description of the rate process and they followed this by a mathematical formulation for plastic deformation of crystal materials. In their most recent recovery–athermal glide creep model [71], the distribution of dislocation link lengths is taken into account (this is a refinement of their earlier link-length distribution models [68–70]). This model provides a clear physical picture of the three-dimensional dislocation network and its crystal orientation and has a number of features that give the model considerable predictive capability. The model has been applied to a single-phase austenitic steel and has been shown to be able to simulate a large number of the characteristics of both primary and steady state creep. Both the stress and temperature dependencies of the model have been evaluated.

In this dislocation link-length distribution model [71], the creep process is considered to consist of the following three subprocesses which take place in the dislocation network: (i) by climb-controlled shrinkage of small meshes and growth of large meshes, the average mesh size will increase (recovery process, r); (ii) under the action of the applied stress, the growing dislocation links will be released by the breakage of junctions in the network, when they have attained an appropriate length ($\lambda \geqslant \lambda_{th}$); the released links expand to loops by glide and thereby generate creep strain (release process, s_1); and (iii) the expanding loops will be blocked and partitioned into shorter links by adjacent parts of the network, which become immobile again. New shorter links are then supplied (supply process, s_2).

The three-dimensional dislocation network during creep deformation is characterized by a distribution function $\phi(\lambda, t)$. The creep strain is generated by glide of released links (release process, s_1). The released links can be any dislocation link with a length longer than the threshold link length, λ_{th} (see Fig. 1). These are the mobile dislocations ($\lambda \geqslant \lambda_{th}$) whereas the immobile (network) dislocations are those with lengths between 0 and λ_{th}. The significance of the threshold link length will be discussed later. This threshold link length is given by the expression [71]

$$\lambda_{th} = \frac{2\mu b}{\sigma} \quad (16)$$

The dislocation dynamics during creep can be described according to the above three subprocesses through a set of partial differential equations, including the structure evolution (link-length distribution) equation and the kinetics (creep strain rate) equation,

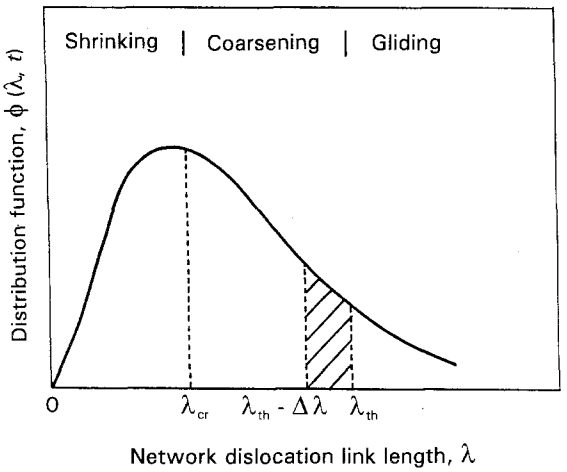

Figure 1 Schematic illustration of distribution function, $\phi(\lambda, t)$, with a critical link length, λ_{cr}, and a threshold link size, λ_{th}, for a typical dislocation link distribution during creep deformation. Dislocation links with lengths $\lambda \geqslant \lambda_{th}$ will glide and thereby produce strain. The glide links are eventually held up (blocked) by adjacent network and new shorter links are then supplied. Links shorter than λ_{th} will undergo recovery, whereas links longer than λ_{cr} will grow until they become mobile ($\lambda \geqslant \lambda_{th}$), and shorter ones ($\lambda < \lambda_{cr}$) will shrink and disappear ($\lambda \to 0$).

and their corresponding boundary conditions for network geometry. During creep deformation, the distribution function will vary and allow the shorter links ($\lambda < \lambda_{cr}$) to shrink and the longer links ($\lambda_{cr} < \lambda < \lambda_{th}$) to grow as well as the links where $\lambda \geqslant \lambda_{th}$ to glide (see Fig. 1). The first two processes, i.e. shrinkage and growth, of the individual links were assumed to follow the network coarsening kinetic equation analogous to the grain growth theory [34, 35, 72–74] (Ostwald ripening mechanism [75–78])

$$\frac{d\lambda}{dt} = M\Gamma\left(\frac{1}{\lambda_{cr}} - \frac{1}{\lambda}\right) \tag{17}$$

where $\Gamma = \mu b^2/2$ is the dislocation line tension, and M is the mobility of the climb dislocations. The distribution frequency function $\phi(\lambda, t)$ is defined such that the number of links per unit volume with length from 0–λ is $N(\lambda, t)$ and the total dislocation density is $\rho(t)$ at time t

$$N(\lambda, t) = \int_0^{\lambda} \phi(\lambda, t)\, d\lambda \tag{18}$$

$$\rho(t) = \int_0^{\infty} \lambda\phi(\lambda, t)\, d\lambda \tag{19}$$

The theory then describes the development of the link-length distribution, $\phi(\lambda, t) \equiv \phi$, with time during the creep test and derives all other relevant outputs (including the creep strain rate, the creep strain, the mobile and immobile dislocation density, etc.) from the evolution of this link-length distribution. The governing network structure equation is

$$\frac{\partial\phi}{\partial t} = \left(\frac{\partial\phi}{\partial t}\right)_r + \left(\frac{\partial\phi}{\partial t}\right)_{s_1} + \left(\frac{\partial\phi}{\partial t}\right)_{s_2} \tag{20}$$

On the right-hand side of Equation 20, the subscripts r, s_1 and s_2 represent recovery, release gliding process and supply process, respectively. The last two terms constitute the strain process, $s = s_1 + s_2$. The three terms on the right-hand side of Equation 20 are as follows [71]

$$\left(\frac{\partial\phi}{\partial t}\right)_r = -\left(\frac{d\lambda}{dt}\frac{\partial\phi}{\partial\lambda} - \frac{M\Gamma}{\lambda^2}\phi\right) \tag{21}$$

$$\left(\frac{\partial\phi}{\partial t}\right)_{s_1} = -H(x)\frac{q-1}{\lambda}\frac{d\lambda}{dt}\phi(\lambda, t) \tag{22}$$

$$\left(\frac{\partial\phi}{\partial t}\right)_{s_2} = c(t)\lambda\left\{\frac{3}{k^2(t)}\phi\left[\frac{\lambda}{k(t)}, t\right] - \phi(\lambda, t)\right\} \tag{23}$$

where $H(x)$ is the Heaviside unit function defined by $H(x) = 1$ when $x \geqslant 0$ and $H(x) = 0$ when $x < 0$; $x = \lambda - \max(\lambda_{cr}, \lambda_{th})$; q is an orientation constant which determines the distribution of links in the different slip systems and is larger than 2; and $c(t)$ is the probability function in the supply process. The probability that a link of length λ will be hit by an expanding loop during the time interval $(t, t + \Delta t)$ is equal to $c(t)\lambda\Delta t$. $k(t)$ is the network geometry factor in the supply process whose value is less than 1 [71].

The recovery coarsening process increases average link length and decreases total dislocation density, whereas the strain process (virtually only the release process, s_1) increases the total dislocation density. In steady state, these two processes (r and s) balance each other dynamically, and the distribution function becomes a steady state distribution (time independent). During the entire creep process, from primary to steady state, the change of the three-dimensional network is always restricted by the constant volume of the creep specimen. Both the recovery process and the strain process should meet this constant volume condition, namely

$$\int_0^{\infty} \lambda^3\left(\frac{\partial\phi(\lambda, t)}{\partial t}\right)_r d\lambda = \int_0^{\infty} \lambda^3\left(\frac{\partial\phi(\lambda, t)}{\partial t}\right)_s d\lambda = 0 \tag{24}$$

In the recovery process the volume conservation condition determines the value of $\lambda_{cr}(t)$:

$$\lambda_{cr}(t) = \frac{\int_0^{\infty} \lambda^2\phi(\lambda, t)\, d\lambda}{\int_0^{\infty} \lambda\phi(\lambda, t)\, d\lambda} \tag{25}$$

The strain rate kinetic equation is obtained by assuming the expanded dislocation loops are circular with an average radius, r

$$\frac{d\varepsilon}{dt} = -\frac{\pi r^2 b}{m}\int_0^{\infty}\left(\frac{\partial\phi(\lambda, t)}{\partial t}\right)_{s_1} d\lambda \tag{26}$$

and the dislocation density change in the strain process is given by

$$\frac{d\rho}{dt} = -(2\pi r)\int_0^{\infty}\left(\frac{\partial\phi(\lambda, t)}{\partial t}\right)_{s_1} d\lambda \tag{27}$$

where m is the Taylor factor. For fcc metals, $m = 3.1$ [79]. The contribution of the release expanding process, s_1, to the creep strain rate and dislocation density is seen in the kinetic Equation 26 and Equation 27, respectively. It has been demonstrated that the climb

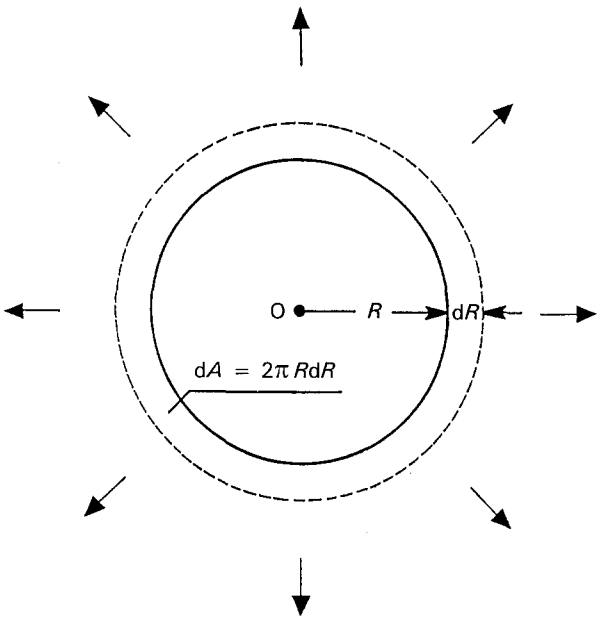

Figure 2 Schematic diagram showing outwards expansion of pure edge dislocation loop for a larger one by diffusion climb. The radius of the loop has increased dR during a time interval dt, and the area swept out is dA. Smaller loops will shrink inwards and disappear. This recovery climb process is a basic event in the dislocation network models of recovery creep deformation at elevated temperatures ($T \geqslant 0.5T_m$, where T_m is the melting temperature measured in degrees Kelvin).

process of the network will not generate a creep strain [80]. This was shown by using a network model where the climb process is visualized as the expansion or shrinkage of a pure edge dislocation loop, Fig. 2. The supply process, s_2, is a process where the expanding loop is eventually arrested by the adjacent network, in this process new shorter links are then supplied. It is obvious that this process will neither produce creep strain nor will it change the dislocation density.

In deriving the release term (the second term on the right-hand side of Equation 20), a quantity $\omega = 1/m$ is introduced which is the inverse of the Schmid factor. For polycrystalline materials deforming plastically at high temperatures, the quantity, ω, can be regarded as a continuous variable. This is physically justifiable [71]. First, in a polycrystalline specimen the total number of slip systems is very large, which is equal to the number of grains times the number of slip systems in each grain. Secondly, ω is defined as the inverse of the Schmid factor, that is the ratio between the applied tensile stress and the resolved shear stress, $\omega = \sigma/\tau_j$. However, the shear stress, which is actually acting upon a dislocation link, is not exactly equal to τ_j because fluctuating internal stresses exist in the crystal. For an individual slip system, the ω values will then be spread out continuously. Then, each dislocation link is associated with both an ω value (slip system and its crystal orientation) and a λ value (link length). Because $m \leqslant 1/2$, one has $\omega \geqslant 2$. Arrested links satisfy $\omega > \sigma\lambda/\mu b$ and mobile links satisfy $\omega \leqslant \sigma\lambda/\mu b$, where the resolved shear stress $\tau_j = m_j\sigma$ (m_j is the Schmid factor for an individual slip system j) in the jth slip system is either less or larger than the average shear stress, τ_{FR}. This τ_{FR} is required for a dislocation link to be released by the operation of the Frank–Read mechanism [81], where $\tau_{FR} = \mu b/\lambda$ is the Frank–Read threshold stress. The shortest link that can be released for a given applied stress, σ, is obtained from $\lambda \geqslant \mu b/m_j\sigma$ (for mobile links) by inserting the maximum value of the Schmid factor, which is 1/2. Therefore, links shorter than $\lambda_{th} = 2\mu b/\sigma$ cannot be released. Both the existence and the stress dependence of λ_{th} have been proved in the model [71].

Equations 20–27 have been solved numerically for the creep deformation of a 20% Cr–35% Ni austenitic stainless steel. The calculated creep strain, dislocation density, and strain-hardening coefficient for both primary and steady-state agree well with experimental results for the material. Also, the model [71] shows that the decrease of the strain rate and the large increase in strain-hardening coefficient during the primary stage are caused by the same phenomenon, namely that only links longer than λ_{th} given by Equation 16, $\lambda_{th} = 2\mu b/\sigma$, can be released and start to glide, thereby producing creep strain, and the number of these long links is gradually exhausted during the primary creep stage. The high value of the steady-state strain-hardening coefficient (of the order of shear modulus) is explained by this result. The steady-state dislocation density and its stress dependence are largely determined by the threshold link length, λ_{th} [71]. The calculated value for strain-hardening coefficient in steady-state, i.e. $H = 0.62\mu$, is typical of steady-state creep where experimental values between 0.2μ and 1.6μ have been reported for a number of materials [17, 19, 20, 82, 83]. It is also consistent with predictions of Evan's strain-hardening model [53]. Another important result is that the model [71] predicts an incubation time with zero strain rate, Δt, and an instantaneous strain, $\Delta\varepsilon$, for an arbitrary stress decrement, $-\Delta\sigma$, and increment, $+\Delta\sigma$, respectively. These two quantities, Δt and $\Delta\varepsilon$, can be calculated from the distribution function, ϕ, and the threshold link length, λ_{th}, for a stress change test during creep deformation.

Lagneborg's creep theory [71], especially the sections dealing with the evolution of the distribution function, ϕ, the threshold link length, λ_{th}, and the stress change behaviour, Δt, $\Delta\varepsilon$, $\pm\Delta\sigma$, has been the foundation and starting point for a number of other models and studies, which we will now examine. For example, the stress-change tests can be used to determine strain-hardening coefficient during steady-state creep [82]. Also, the shape of the strain transient following a sudden stress change (drop or increment) during steady-state creep provides a useful experimental technique for probing the micromechanisms of creep [9]. The shape of the strain transient after a stress increase during steady-state creep is a reliable indicator of the rate-controlling mechanism of creep. Metals and alloys in which recovery is the rate-controlling mechanism (i.e. pure metals and Class II alloys) exhibit an N-type (normal) transient for which the initial creep rate is high, but decreases with time reaching a constant or "steady state" value. Class I alloys, in which viscous glide is rate controlling, exhibit an I-type (invert) transient for which the creep rate gradually increases to reach a constant value. The

shape of the strain transient after a sudden stress drop, on the other hand, gives no immediate indication of the rate-controlling mechanism in creep, because pure metals and Class I and Class II alloys each show I-type transient. However, the stress drop test can still be invaluable in determining such quantities as effective stress, internal stress [10], and the recovery rate [15–20] in steady-state creep.

3.2. Ardell and Przystupa's link-length statistics model

Ardell and Przystupa [84] have developed a theory of elevated-temperature deformation, based on the statistics of the distribution of dislocation link lengths. The distribution consists of a sessile region ($\lambda < \lambda_{th}$), in which network growth, or recovery, occurs by a coarsening process, and a glissile region ($\lambda \geqslant \lambda_{th}$), in which dislocation links are long enough to glide (here λ_{th} is a critical link length determined by the applied stress). A major premise of this theory is that network coarsening continually produces a supply of links that grow and exceed λ_{th}. These links can then move in an unconstrained manner until they collide with shorter links in the network, thereby stimulating the coarsening process anew. Steady-state deformation is possible when network coarsening and refinement balance each other in such a way that $\phi(\lambda, t)$ becomes independent of time [84]. Partial differential equations governing the evolution of the distribution of link lengths have been obtained for a model that assumes gliding links collide only with network links and produce only new network links. The total change in the number of links in the size interval between λ and $\lambda + d\lambda$ is given by the equation

$$\frac{\partial \phi}{\partial t} = -\frac{\partial(\phi g)}{\partial \lambda} + \sum_{i=1}^{n} Q_i(\lambda, t) \quad (28)$$

where $g = g(\lambda, t) \equiv d\lambda/dt$ is the growth rate of an individual link of length λ; $Q_i(\lambda, t) = \delta\phi_i(\lambda, t)/\delta t$, where $\delta\phi_i(\lambda, t)d\lambda$ is the number of links per unit volume added to the interval λ, $\lambda + d\lambda$ from the ith source in the time interval δt; and n is the total number of sources contributing to the formation of new links. Four source terms $Q_i(\lambda, t)$ have been analysed [84]. For the region $0 < \lambda < \lambda_{th}$, there are three source terms: namely (i) $Q_1(\lambda, t)d\lambda$ which accounts for the new links with length between λ and $\lambda + d\lambda$ that are produced by division of network links having length $\lambda < \lambda' < \lambda_{th}$; (ii) $Q_2(\lambda, t)d\lambda$ which accounts for the links which leave the interval λ, $\lambda + d\lambda$ during the collision process; and (iii) $Q_3(\lambda, t)d\lambda$ which is the contribution to λ, $\lambda + d\lambda$ form the network links produced by division of the gliding links. For the region $\lambda > \lambda_{th}$ there is only one source: namely $Q_4(\lambda, t)d\lambda$ which results from the loss of links from an interval in this region. These four sources are defined as follows [84]

$$Q_1(\lambda, t) = \frac{2M}{N_n}\int_{\lambda}^{\lambda_{th}} \frac{\phi(\lambda', t)}{\lambda'} d\lambda' \quad (29)$$

$$Q_2(\lambda, t) = -\frac{M}{N_n}\phi(\lambda, t) \quad (30)$$

$$Q_3(\lambda, t) = \frac{M_d}{N_n}(j + 1)\phi(\lambda, t) \quad (31)$$

$$Q_4(\lambda, t) = -p(\lambda, t)g_g\phi(\lambda, t) \quad (32)$$

where M is the rate of collisions per unit volume of the network lines by gliding links; N_n is the number of network links per unit volume in the sessile region $(0, \lambda_{th})$, M_d is the total rate per unit volume at which gliding links encounter network links, $(j + 1)$ is the number of network links per unit volume created by a gliding link which collides on average with j network links; $p(\lambda, t)$ is the probability that a gliding link encounters several network links per unit volume; and g_g is equal to $d\lambda/dt$ in the glissile region (λ_{th}, ∞) [84].

Each collision between two links results in their destruction and the formation of four new shorter links, regardless of the type of collision [68, 84]. If M is the rate of collisions per unit volume, and the total rate of formation of new links per unit volume is $2M$, then

$$\sum_{i=1}^{n}\int_{0}^{\infty} Q_i(\lambda, t)d\lambda = 2M \quad (33)$$

A general expression for the rate at which the number of links per unit volume changes with time, dN/dt, is given by

$$\frac{dN}{dt} = \lim_{\lambda \to 0}(\phi g) + 2M \quad (34)$$

The first term is equivalent to the statement that a link can disappear only by shrinking to zero size. Because the total length of the links remains unchanged during the collision process, then we can write

$$\sum_{i=1}^{n}\int_{0}^{\infty} \lambda Q_i(\lambda, t)d\lambda = 0 \quad (35)$$

The rate at which the dislocation density changes with time can be described by

$$\frac{d\rho}{dt} = N\langle g\rangle \quad (36)$$

which implies that the kinetics of dislocation multiplication and annihilation are controlled entirely by the factors that govern the average rate of link growth. Equations 33–36 constrain the behaviour of $\phi(\lambda, t) \equiv \phi$, and are the boundary conditions for Equation 28.

The self-consistency of the theory [84] has been analysed with respect to the model Equations 28–36. Ardell and Przystupa demonstrated analytically that the values of dN/dt and $d\rho/dt$ predicted by the continuity Equation 28 with all the source terms $Q_i(\lambda, t)$ are consistent with the conservation Equations 33–35, respectively.

The strain rate obtained from this model is given by the expression

$$\dot{\varepsilon} = \alpha \boldsymbol{b} r \beta \sin^2[\langle\lambda_n\rangle/(2r)]\langle g_n\rangle N_n + \alpha \boldsymbol{b} q v \rho_g \quad (37)$$

where r is radius of a bowing out network link λ_n, $\beta = \beta(t)$ is a constant dependent upon the shape of the distribution, the subscripts n and g represent network

and glide links, respectively, q is a geometrical constant and $v = dr/dt$ is the velocity of the gliding links. This strain rate, Equation 37, predicts automatically, without *ad hoc* assumptions, that there is a recovery component (the first term from constrained motion) and a glide component (the second term from unconstrained motion: "free motion") contributing to the strain rate. In this sense this present theory justifies the earlier hypothesis of Ajaja and Ardell [85] that the annihilation of dislocations generates creep strain. This contribution is found to be very significant when recovery is appreciable, and is mainly responsible for the decreasing creep rate associated with the normal primary creep of Class II materials [85]. It is also supported by recent experimental results, which clearly show that both static and dynamic recovery can produce significant strain [85, 86].

Some implications in high-temperature creep of Class II materials have been also discussed in terms of this model [84]. The dislocation multiplication and annihilation kinetics are found to be similar to the earlier one [87–90], i.e.

$$\frac{d\rho}{dt} = k_1\rho - k_2\rho^2 \tag{38}$$

with two important exceptions: namely (i) the rate constants k_1 and k_2 are time dependent; and (ii) the multiplication rate is proportional to $\rho^{3/2}$ rather than ρ, whereas the annihilation rate remains proportional to ρ^2. Transient creep and the initial creep rate have also been analysed and it is shown that the initial stages of creep of Class II materials are controlled by the network growth process (dislocation glide in the conventional sense contributing almost nothing to the deformation), and that the phenomenon of recovery produces positive strain in the sample. For steady-state creep, the model predicts that $\dot{\varepsilon}_s$ is governed quite generally by the Taylor–Orowan equation [14, 51, 52, 91–95], namely

$$\dot{\varepsilon} = \alpha \boldsymbol{b} \rho_m v \tag{39}$$

modified realistically by a "microstructural parameter", S, which depends upon the dislocation microstructure through the nature of the dislocation link-length distribution. It has long been recognized that a microstructural parameter should influence the steady-state creep rate of different materials [1, 96], and such parameters have been introduced into various theories on an *ad hoc* semi-empirical basis. In this theory, it arises naturally through the influence that microstructural factors (e.g. crystal structure, stacking fault energy) have on the shape of the dislocation link-length distribution and on the values of the fraction of mobile dislocation density and the fraction of mobile dislocation links in steady-state. It is also pointed out that the model results in a steady-state creep rate, $\dot{\varepsilon}_s$, equation which is consistent with the so-called "natural law" [97–100], $\dot{\varepsilon}_s \propto \sigma^3$, which arises when $v \propto \sigma$ and $\rho_s \propto \sigma^2$. Here, however, stress exponents greater than 3 can result from the "potential" stress dependence of the structural parameter S.

This model [84] has also been modified successfully to account for the experimental observation [101] that none of the links in the distribution of dislocation link lengths in monocrystalline aluminium deformed in compression at 920 K is long enough to glide or climb in an unconstrained manner [102]. That is, in Harper–Dorn creep [103, 104] there is no free glide, but rather there is climb-assisted glide (constrained motion) of dislocation links in the network coarsening dynamics which will generate a finite strain rate. When the applied stress is high enough, such as in the power law regime, some links have lengths larger than λ_{th}, and a dislocation segment can move by either climb or glide, or a combination of both, without the need to remain in equilibrium with its line tension (this line tension relates to unconstrained motion). In the Harper–Dorn (H–D) creep regime, for all links with length $\lambda < \lambda_{th}$, the dislocation must move somehow if it is to adjust its length when its pinning points (the nodes in the network) move as the network coarsens. This movement must necessarily also occur by small increments of glide or climb, or a combination of both, but such motion is constrained by the requirement that the forces acting on the dislocation and impelling its motion are always in equilibrium with its line tension [102]. The continuity equation for steady-state H–D creep is the second-order differential equation (modified from Equation 28) given by

$$\frac{d^2J_s}{d\lambda^2} + \frac{2M_{ns}}{N_{ns}}\frac{d\phi_s}{d\lambda} + \frac{4M_{ns}}{N_{ns}}\frac{\phi_s}{\lambda} = 0 \tag{40}$$

where $J = \phi g$, and the subscript s indicates the steady state value of the respective parameters and functions. The steady-state creep strain predicted by this modified model [102] for H–D creep conditions is approximately given by

$$\dot{\varepsilon}_s \approx \frac{\alpha M_{ns} \boldsymbol{b}^2 \langle \lambda_s^3 \rangle}{24\Gamma}\sigma \tag{41}$$

which predicts that steady-state H–D creep is Newtonian in the limit of small applied stress, as is observed experimentally. The temperature dependence of $\dot{\varepsilon}_s$ is contained primarily in the parameter M_{ns} (the rate per unit volume of collisions between constrained links), which is logically governed by diffusion. Some contribution from the factor $\langle(\lambda_s)^3\rangle$ can be expected if the shape of the link-length distribution is temperature dependent during steady-state H–D creep [102].

3.3. Ajaja's link-length distribution analysis

Recently, Ajaja has analysed recovery creep [105], the Bailey–Orowan equation [106], and the role of recovery in high-temperature constant strain-rate deformation [107], using a model based on the three-dimensional distribution of dislocation links. In a recovery creep model [105], the jerky glide motion of dislocations between obstacles is assumed. A three-dimensional distribution of dislocation links is visualized such that only links which attain a certain threshold size through recovery can glide rapidly until they are again arrested at the next obstacle. It is shown that the rate of mobilization, $\dot{\rho}_m$, of arrested dislocations is directly proportional to the annihilation rate, $\dot{\rho}_a$, i.e. $\dot{\rho}_m = \psi(t)\dot{\rho}_a$. The creep strain rate, $\dot{\varepsilon}$, during

transient creep is related to the annihilation rate, $\dot{\rho}_a$, the obstacle spacing, L, and the Burgers vector $\boldsymbol{b}$ of the dislocations according to the expression

$$\dot{\varepsilon} = \alpha_1 \psi(t)\, \dot{\rho}_a \boldsymbol{b} L \tag{42}$$

where α_1 is a geometrical constant, $\psi(t)$ is a time-dependent parameter which is determined by the instantaneous free dislocation density as well as the dislocation distribution. At steady-state, $\psi(t)$ becomes a constant which is stress and temperature independent.

The average effective dislocation velocity is also shown to be linearly proportional to the annihilation rate, $v = [\psi(t)\rho^{-3/2}]\dot{\rho}_a$. This relation shows that v is not a "glide" velocity *per se*, because its value is determined more by the rate of release of arrested dislocations than by the details of the glide process itself [105]. This model has demonstrated clearly the prominent role played by two major factors during crystal deformation, see Equation 42. The first, and the more familiar one, is the number density of obstacles, which is important to the extent that it determines the inter-obstacle spacing between which a released dislocation link can glide freely. The second, and perhaps more important factor, is the rate of release of arrested dislocations. During the creep of pure metals, the former is determined by the dislocation density, and the latter by the rate of recovery. Also in this model it is argued that the incorporation of subgrain strengthening to explain transient creep behaviour [108] (the decreasing creep rate in normal primary creep) is not justified by recent experimental results [109, 110], and is considered not necessary in the light of the model. However, further development of the model is needed, because the details of the annihilation rate process and evolution of the dislocation link length distribution have not been considered in the model so far developed.

The above model [105] has been employed to analyse the use of stress change test technique in measuring recovery rate, R, and strain-hardening coefficient, H, and the derivation of the Bailey–Orowan equation, $\dot{\varepsilon} = R/H$. It is demonstrated [106] that this equation is valid for steady-state but not for transient creep which is essentially in agreement with Bailey's original model [13], and that the values of R_m and H_m which are measured by stress change techniques do not represent the true values of the recovery rate, R, and strain-hardening coefficient, H. However, the ratio of the measured values is always equal to the strain rate during transient and steady state, that is [106]

$$\dot{\varepsilon} = \frac{R_m}{H_m} \tag{43}$$

which agrees the early analysis and experimental measurements made by Barrett *et al.* [111]. In terms of the true values of R and H, the creep rate during transient creep is given by

$$\dot{\varepsilon} = \beta\psi(t)\frac{R}{H} \tag{44}$$

which clearly shows that the Bailey–Orowan equation is not applicable to transient creep. In Equation 44, β is a constant whose value depends mainly on the link geometry during glide, and $\psi(t)$ is a time-dependent parameter related to dislocation distribution. In steady-state, where $\beta\psi(t) = 1$, the Bailey–Orowan equation is easily obtained from Equation 44. In steady-state there is a true balance between the recovery and strain-hardening processes.

The model [105] has also been used to delineate the role of recovery during high temperature constant strain rate deformation [107]. It is shown that the model provides a good semi-quantitative explanation for classical strain-hardening as well as for high-temperature strain-softening resulting from rapid recovery. It predicts linear strain-hardening, whereby the ratio of the strain-hardening coefficient, H, to the shear modulus, μ, is constant when a crystal is tested in the absence of recovery. The slope of the stress–strain curve, Θ, for high-temperature constant strain-rate deformation is related to the low-temperature strain-hardening coefficient, H, the dislocation annihilation rate, $\dot{\rho}_a$, the flow stress, σ, the free dislocation density, ρ, the strain rate, $\dot{\varepsilon}$, and a parameter which is sensitive to the dislocation distribution. The model gives a modified version of the Bailey–Orowan equation for simultaneous strain-hardening and recovery during constant strain-rate deformation, namely

$$\Theta = H - \eta(t)\frac{R}{\dot{\varepsilon}} \tag{45}$$

where R is the recovery rate, H is the low-temperature strain-hardening coefficient, $\eta(t)$ is time dependent during transient stage of deformation, which is determined by such factors as σ, ρ and details of the dislocation distribution, i.e. $\eta(t) = \alpha_0\psi_0\sigma^2/(\alpha_2 c^2 \rho)$, where α_0 and α_2 are constants, ψ_0 is the ratio of the growth rate of threshold-size links, λ_{th}, to the growth rate of the average link size, $\langle\lambda\rangle$ [105], $c = \alpha_0\mu\boldsymbol{b}$. In steady-state stage, $\eta(t) \equiv 1$ which gives a direct proportionality between σ and $\rho^{1/2}$ as is required by strain-hardening models, i.e. $\sigma = \alpha_3\mu\boldsymbol{b}\rho^{1/2}$, where $\alpha_3 = (\alpha_0\alpha_2/\psi_0)^{1/2}$ is a constant. Equation 45 has been applied to the experimental results for NaCl monocrystals deformed under compression at 873 and 973 K [112]. The calculated strain-hardening coefficient, H, is in fair agreement with other reported results [113, 114]. It is also shown in this analysis that a direct correlation exists between the recovery rate, R, and the dislocation density, ρ, whereby the larger the dislocation density the higher the recovery rate.

4. Discussion and conclusion

As has been pointed out by Lagneborg [26], there are a number of widely accepted theories for creep deformation by recovery creep. These include Weertman's dislocation climb models [97, 115, 116], models based on thermally activated motion of jogged screw dislocations [97, 117–120], and models based on the climb process of extended dislocations [121–124]. These theories have cast light upon the climb recovery, and dislocation dynamics in dislocation creep,

and are consistent with the experimental results on both the activation energy and stress exponent of steady-state creep rate and the stacking fault energy effect [1]. However, the drawbacks of these models are also well-known, e.g. whether dislocations on parallel slip planes and of opposite sign will be held up by mutual interaction and form pile-ups as in the climb model [125]. The imperfections of the dislocation-jog model are in many respects similar to those of the climb theory [26]. For example, the uncertainty of the mobile dislocation density, ρ_m, is great, with respect both to its magnitude and stress-dependence. Furthermore, the stress-dependence of the spacing between the jogs is not considered. On the other hand, the network models especially the recent ones, are based upon a detailed description of the evolution of the distribution function for the dislocation network structure as a three-dimensional distribution of link lengths, and are far more appealing on physical grounds. One of the principal advantages of such models is that out of all the existing dislocation links, it automatically and in a physically-sound fashion "selects" the few mobile links when it comes to deriving the creep strain rate.

There are, however, one or two approximations made in the dislocation link distribution models, which relate to the subgrain formation and the network recovery kinetics. The first assumption is that distribution frequency function $\phi(\lambda, t)$ only takes into account those free dislocation links not incorporated in subgrain boundaries. It now seems that this is a justifiable approximation from the point of view of Li's elastic theories of subgrain boundaries [126–129] and recent experimental observations on high-temperature deformation [130–136]. A uniform array of dislocations is inherently energetically unstable and tends to form a modulated cell structure [137, 138]. High-temperature deformation of an Al–Mg–Mn alloy has been carried out [136] in plane-strain compression at constant strain rate and temperature, and with abrupt changes in the Zener–Hollomon parameter, $Z = \dot{\varepsilon} \exp(\Delta H/RT)$, where ΔH is activation enthalpy [139–141]. It was found that the proof strength depends primarily on the dislocation density within the subgrains [136]. The subgrain size played a lesser role. This is interpreted in terms of the fact that dislocations within boundaries have a lower strengthening efficiency per dislocation. The lesser role of the subgrain size can be considered in terms of a Hall–Petch contribution [142–145] with the subgrain-boundary strength being much less than the strength of grain boundaries [136]. In fact, experiments show that characteristic networks of dislocations tend to form in creep. The network outline cells within which there are relatively few free dislocations. As the networks do not exert significant long-range stresses, most of the free dislocations within the cells are unaffected by the stresses produced by dislocations in the cell walls [35]. They are, however, subject to the internal stress produced by the line tension of the dislocation link itself [146]. The stable subgrain boundaries have no long-range stresses. Because the effects of the array are all short-range in nature, it can be said that an infinite edge dislocation array is a weaker barrier for the penetration of parallel edge dislocations than the same set of edge dislocations which composed the array but are distributed randomly [129]. Also, because the flow stress stays nearly constant, the dramatic changes in the character of the subgrain boundaries that are observed during steady-state deformation suggest that the details of the sub-boundaries are not an important consideration in the rate-controlling process for creep, and as such any description of the rate-controlling process for creep should consider the density of dislocations not associated with subgrain boundaries [130–135].

The second assumption relates to the network coarsening kinetics, i.e. Equation 17. It has been pointed out that this equation in its present form cannot fully describe the network coarsening process [71, 102, 147, 148]. However, Equation 17 is, in fact, identical to Friedel's equation for the dislocation link speed of climb for the lines of the networks [35], namely

$$\frac{dr}{dt} = \frac{D_s \mu \boldsymbol{b}^3 C_j}{kT} \frac{1}{r} \tag{46}$$

when one takes the network spacing, r, to be the dislocation link length and sets the mobility, M, and the line tension, Γ, equal to:

$$M = 2C_j D_s \boldsymbol{b}/kT \tag{47}$$

$$\Gamma = \mu \boldsymbol{b}^2/2 \tag{48}$$

where D_s is the atomic self-diffusion coefficient and C_j is the jog concentration [149]. This is the classical Einstein formula [54, 150–152], which in this case relates the drift velocity of the climbing dislocation lines to the atomic self-diffusion coefficient, D_s, and to the force due to the line tension of the dislocations [153–158]. The nature of dislocation network coarsening is to reduce the free energy of the system through a thermal activation process of atomic diffusion. Thus, the universal Einstein equation [152] is applicable to the network-coarsening process in a proper formulation of the rate equations. Plastic deformation of crystalline solids is basically due to thermally activated deformation processes [149, 159–166]. Creep recovery coarsening during creep deformation at elevated temperatures and under an externally applied stress is an extremely complicated dynamic process. Although Equation 17 can describe the basic physical nature of the dislocation network coarsening process during creep deformation, it is unable to predict fully all details of the rate process in network coarsening. Keeping these points in mind, it is therefore clear that the link-length distribution models are only approximate models for recovery creep. Further work should then be concentrated on the role of subgrain formation and on a more accurate description of the network coarsening during high-temperature creep deformation.

Acknowledgement

Financial support for this work from the Natural Science and Engineering Research Council of Canada

through a Research Grant (A4391) to Professor D. O. Northwood is gratefully acknowledged.

References

1. O. B. SHERBY and P. M. BURKE, *Prog. Mater. Sci.* **13** (1968) 323.
2. S. TAKEUCHI and A. S. ARGON, *Acta Metall.* **24** (1976) 883.
3. N. F. MOTT, *Proc. Phys. Soc. London* **64B** (1951) 729.
4. *Idem, Philos. Mag.* **44** (1953) 724.
5. W. R. CANNON and O. D. SHERBY, *Metall. Trans.* **1** (1970) 1030.
6. K. L. MURTY, *Philos. Mag.* **29** (1974) 429.
7. F. A. MOHAMED and T. G. LANGDON, *Acta Metall.* **22** (1974) 779.
8. *Idem, Metall. Trans.* **6A** (1975) 927.
9. D. O. NORTHWOOD and I. O. SMITH, *Metal Sci.* **18** (1984) 485.
10. *Idem, Metals Forum* **8** (1985) 237.
11. J. B. FAGBULU and O. AJAJA, *J. Mater. Sci. Lett.* **6** (1987) 894.
12. G. A. HENSHALL and A. K. MILLER, *Acta Metall. Mater.* **38** (1990) 2101.
13. R. W. BAILEY, *J. Inst. Metals* **35** (1926) 27.
14. E. OROWAN, *J. West Scotland Iron Steel Inst.* **54** (1947) 45.
15. A. H. COTTRELL and V. AYTEKIN, *J. Inst. Metals* **77** (1950) 389.
16. A. H. COTTRELL, in "Dislocations and Plastic Flow in Crystals" (Oxford University Press, London, 1953) p. 195.
17. S. K. MITRA and D. McLEAN, *Proc. Roy. Soc. London* **295A** (1966) 288.
18. *Idem, Metal Sci. J.* **1** (1967) 192.
19. W. J. EVANS and B. WILSHIRE, *Trans. AIME* **242** (1968) 2514.
20. *Idem, Metal Sci. J.* **4** (1970) 89.
21. T. WATANABE and S. KARASHIMA, *ibid.* **4** (1970) 52.
22. G. J. LLOYD and R. J. McELROY, *Acta Metall.* **22** (1974) 339.
23. D. McLEAN, *Rep. Prog. Phys.* **29** (1966) 1.
24. R. LAGNEBORG, *Metal Sci. J.* **3** (1969) 56.
25. J. H. GITTUS, *Philos. Mag.* **23** (1971) 1281.
26. R. LAGNEBORG, in "Creep of Engineering Materials and Structures", edited by G. Bernasconi and G. Piatti (Applied Science, London, 1978) p. 7.
27. F. C. FRANK, in "A Symposium on the Plastic Deformation of Crystalline Solids" (Carnegie Institute of Technology, Mellon Institute, Pittsburgh, PA, 1950) p. 89.
28. D. McLEAN, in "High Temperature Materials: The Controlling Physical Process", edited by A. J. Kennedy (Oliver and Boyd, Edinburgh, London, 1968) p. 7.
29. B. L. JONES and C. M. SELLARS, *Metal Sci. J.* **4** (1970) 96.
30. A. ODÉN, E. LIND and R. LAGNEBORG, in "Proceedings of a Meeting on Creep Strength in Steel and High-Temperature Alloys" (Iron and Steel Institute, London, 1972) p. 60.
31. J. B. BILDE-SÖRENSEN, *Acta Metall.* **21** (1973) 1495.
32. P. LIN, S. S. LEE and A. J. ARDELL, *ibid.* **37** (1989) 739.
33. B. WANG, F. SUN, Q. MENG and W. XU, *Acta Metall. Sinica* **28A** (1992) 100.
34. D. McLEAN, *Trans. AIME* **242** (1968) 1193.
35. J. FRIEDEL, in "Dislocations" (Pergamon, Oxford, 1964) p. 239.
36. E. OROWAN, in "Symposium on Internal Stresses in Metals and Alloys" (Institute of Metals, London, 1948) p. 47.
37. *Idem*, in "Dislocations in Metals", edited by M. Cohen (AIME, New York, 1954) p. 69.
38. F. R. N. NABARRO, Z. S. BASINSKI and D. B. HOLT, *Adv. Phys.* **13** (1964) 193.
39. F. R. N. NABARRO, *Acta Metall.* **37** (1989) 1521.
40. J. H. GITTUS, *ibid.* **22** (1974) 789.
41. F. H. NORTON, in "The Creep of Steel at High Temperatures" (McGraw-Hill, New York, 1929) p. 67.
42. D. McLEAN, *Metall. Rev.* **7** (1962) 481.
43. J. WEERTMAN, *Trans. AIME* **227** (1963) 1475.
44. *Idem, Trans. ASM* **61** (1968) 681.
45. J. E. BIRD, A. K. MUKHERJEE and J. E. DORN, in "Quantitative Relation Between Properties and Microstructure", edited by D. G. Brandon and A. Rosen (Israel University Press, Jerusalem, 1969) p. 255.
46. A. K. MUKHERJEE, J. E. BIRD and J. E. DORN, *Trans. ASM* **62** (1969) 155.
47. R. RAJ and M. F. ASHBY, *Metall. Trans.* **2** (1971) 1113.
48. M. F. ASHBY, *Acta Metall.* **22** (1972) 789.
49. W. D. NIX, J. C. GIBELING and D. A. HUGHES, *Metall. Trans.* **16A** (1985) 2215.
50. B. L. ADAMS and D. P. FIELD, *Acta Metall. Mater.* **39** (1991) 2405.
51. G. I. TAYLOR, *Proc. Roy. Soc. London* **145A** (1934) 362.
52. *Idem, ibid.* **145A** (1934) 388.
53. H. E. EVANS, *Philos. Mag.* **28** (1973) 227.
54. J. H. GITTUS, *Acta Metall.* **22** (1974) 1179.
55. O. D. SHERBY, J. L. LYTTON and J. E. DORN, *ibid.* **5** (1957) 219.
56. C. R. BARRETT and O. D. SHERBY, *Trans. AIME* **230** (1964) 1322.
57. S. L. ROBINSON and O. D. SHERBY, *Acta Metall.* **17** (1969) 109.
58. O. D. SHERBY, *Trans. AIME* **212** (1958) 708.
59. R. LAGNEBORG, *Metal Sci. J.* **6** (1972) 127.
60. H. E. EVANS and G. KNOWLES, *Acta Metall.* **25** (1977) 963.
61. *Idem, ibid.* **26** (1978) 141.
62. R. L. COBLE, *J. Appl. Phys.* **34** (1958) 1679.
63. F. R. N. NABARRO, in "Report of a Conference on the Strength of Solids" (Physics Society, London, 1948) p. 75.
64. C. HERRING, *J. Appl. Phys.* **21** (1950) 437.
65. J. H. GITTUS, *Acta Metall.* **26** (1978) 305.
66. J. D. PARKER and B. WILSHIRE, *Philos. Mag.* **41A** (1980) 665.
67. B. BURTON, *ibid.* **45A** (1982) 657.
68. R. LAGNEBORG, B.-H. FORSÉN and J. WIBERG, in "Proceedings of a Meeting on Creep Strength in Steel and High-Temperature Alloys" (Iron and Steel Institute, London, 1972) p. 1.
69. R. LAGNEBORG and B.-H. FORSÉN, *Acta Metall.* **21** (1973) 781.
70. P. ÖSTRÖM and R. LAGNEBORG, *Trans. ASME J. Eng. Mater. Tech.* **98** (1976) 114.
71. *Idem, Res. Mech.* **1** (1980) 59.
72. M. HILLERT, *Acta Metall.* **13** (1965) 227.
73. I.-W. CHEN, *ibid.* **35** (1987) 1723.
74. C. S. PANDE and E. DANTSKER, *Acta Metall. Mater.* **38** (1990) 945.
75. W. OSTWALD, *Z. Phys. Chem.* **34** (1900) 495.
76. I. M. LIFSHITZ and V. V. SYLOZOV, *J. Phys. Chem. Solids* **19** (1961) 35.
77. C. WAGNER, *Z. Elektrochem.* **65** (1961) 581.
78. J. J. HOYT, *Acta Metall. Mater.* **39** (1991) 2091.
79. U. F. KOCKS, *Metall. Trans.* **1** (1970) 1121.
80. L. SHI and D. O. NORTHWOOD, *Scripta Metall. Mater.* **26** (1992) 777.
81. F. C. FRANK and W. T. READ, *Phys. Rev.* **79** (1950) 722.
82. D. O. NORTHWOOD and I. O. SMITH, *Phys. Status Solidi.* **90A** (1985) 563.
83. F. R. N. NABARRO, *Acta Metall. Mater.* **38** (1990) 637.
84. A. J. ARDELL and M. A. PRZYSTUPA, *Mech. Mater.* **3** (1984) 319.
85. O. AJAJA and A. J. ARDELL, *Philos. Mag.* **39A** (1979) 75.
86. T. HASEGAWA, T. YAKOV and U. F. KOCKS, *Acta Metall.* **30** (1982) 235.
87. W. G. JOHNSTON and J. J. GILMAN, *J. Appl. Phys.* **30** (1959) 129.
88. J. C. M. LI, *Acta Metall.* **11** (1963) 1269.
89. N. S. AKULOV, *ibid.* **12** (1964) 1195.
90. J. C. M. LI, *ibid.* **13** (1965) 37.
91. E. OROWAN, *Proc. Phys. Soc. London* **52** (1940) 8.
92. A. S. KRAUSZ and H. EYRING, in "Deformation Kinetics" (Wiley, New York, 1975) p. 190.

93. U. F. KOCKS, A. S. ARGON and M. F. ASHBY, *Proc. Mater. Sci.* **19** (1975) 88.
94. G. M. PHARR and W. D. NIX, *Acta Metall.* **27** (1979) 433.
95. R. M. CADDELL, in "Deformation and Fracture of Solids" (Prentice-Hall, Englewood Cliffs, NJ, 1980) p. 160.
96. B. WALSER and O. D. SHERBY, *Scripta Metall.* **16** (1982) 213.
97. J. WEERTMAN, in "Rate Processes in Plastic Deformation of Materials", edited by J. C. M. Li and A. K. Mukherjee (ASM, Metals Park, OH, 1975) p. 315.
98. Z. HORITA and T. G. LANGDON, *Scripta Metall.* **17** (1983) 665.
99. S. STRAUB and W. BLUM, *Scripta Metall. Mater.* **24** (1990) 1837.
100. P. A. TIBBITS, *Acta Metall. Mater.* **39** (1991) 105.
101. S. LEE and A. J. ARDELL, in "Strength of Metals and Alloys", Vol. 1, edited by H. J. McQueen, J.-P. Boilon, J. I. Dickson, J. J. Jonas and M. G. Akben (Pergamon, Oxford, 1985) p. 671.
102. A. J. ARDELL and S. S. LEE, *Acta Metall.* **34** (1986) 2411.
103. J. HARPER and J. E. DORN, *ibid.* **5** (1957) 654.
104. F. R. N. NABARRO, *ibid.* **37** (1989) 2217.
105. O. AJAJA, *J. Mater. Sci.* **21** (1986) 3351.
106. S. O. OJEDIRAN and O. AJAJA, *ibid.* **23** (1988) 4037.
107. O. AJAJA, *ibid.* **26** (1991) 6599.
108. O. D. SHERBY, R. H. KLUNDT and A. K. MILLER, *Metall. Trans.* **8A** (1977) 843.
109. O. AJAJA and A. J. ARDELL, *Philos. Mag.* **39A** (1979) 65.
110. J. L. ADELUS, V. GUTTMAN and V. D. SCOTT, *Mater. Sci. Eng.* **44** (1980) 195.
111. C. R. BARRETT, C. N. AHLQUIST and W. D. NIX, *Metal Sci. J.* **4** (1970) 41.
112. M. A. PRZYSTUPA, P. LIN, A. J. ARDELL and O. AJAJA, *Mater. Sci. Eng.* **92** (1987) 63.
113. H. M. OTTE and J. J. HERN, *Exp. Mech.* **6** (1966) 177.
114. W. in der SCHMITTEN and P. HAASEN, *J. Appl. Phys.* **32** (1961) 1790.
115. J. WEERTMAN, *ibid.* **26** (1955) 1213.
116. *Idem, ibid.* **28** (1957) 362.
117. N. F. MOTT, in "Proceedings of a Symposium on the Creep and Fracture of Metals at High Temperatures", NPL, Teddington, May 1954 (HMSO, London, 1957) p. 21.
118. P. B. HIRSCH and D. H. WARRINGTON, *Philos. Mag.* **6** (1961) 735.
119. L. RAYMOND and J. E. DORN, *Trans. AIME* **230** (1964) 560.
120. C. R. BARRETT and W. D. NIX, *Acta Metall.* **13** (1965) 1247.
121. A. S. ARGON and S. TAKEUCHI, *ibid.* **29** (1981) 1877.
122. G. GOTTESTEIN and A. S. ARGON, *ibid.* **35** (1987) 1261.
123. W. XU and Q. P. KONG, *Philos. Mag.* **56A** (1987) 433.
124. Q. P. KONG and Y. LI, *Phys. Status Solidi* **126A** (1991) 129.
125. F. GAROFALO, in "Fundamentals of Creep and Creep-Rupture in Metals" (Macmillan, New York, 1965) p. 188.
126. J. C. M. LI, *Acta Metall.* **8** (1960) 296.
127. *Idem, J. Appl. Phys.* **32** (1960) 1873.
128. J. C. M. LI and C. D. NEEDHAM, *ibid.* **31** (1960) 1318.
129. J. C. M. LI, in "Electron Microscopy and Strength of Crystals", edited by G. Thomas and J. Washburn (Wiley, New York, 1962) p. 713.
130. M. E. KASSNER, *J. Mater. Sci.* **25** (1990) 1997.
131. M. E. KASSNER, J. W. ELMER and C. J. ECHER, *Metall. Trans.* **17A** (1986) 2093.
132. M. E. KASSNER, A. K. MILLER and O. D. SHERBY, *ibid.* **13A** (1982) 1977.
133. O. AJAJA and A. J. ARDELL, *Scripta Metall.* **11** (1977) 1089.
134. T. G. LANGDON, R. B. VASTAVA and P. YAVARI, in "Strength of Metals and Alloys", Vol. 1, edited by P. Haasen, V. Gerold and G. Kostorz (Pergamon, Oxford, 1979) p. 271.
135. M. E. KASSNER and M. E. McMAHON, *Metall. Trans.* **18A** (1987) 835.
136. F. R. CASTRO-FERNÁNDEZ and C. M. SELLARS, *Philos. Mag.* **60A** (1989) 487.
137. D. L. HOLT, *J. Appl. Phys.* **41** (1970) 3197.
138. B. ILSCHNER, in "Constitutive Equations in Plasticity", edited by A. S. Argon (MIT Press, Cambridge, MA, 1975) p. 469.
139. C. ZENER and J. H. HOLLOMON, *J. Appl. Phys.* **15** (1944) 22.
140. *Idem, Trans. ASM* **33** (1944) 163.
141. C. ZENER, *Trans. AIME* **167** (1946) 155.
142. E. O. HALL, *Proc. Phys. Soc. London* **64B** (1951) 747.
143. N. J. PETCH, *J. Iron Steel Inst.* **173** (1953) 25.
144. R. W. ARMSTRONG, I. CODD, R. M. DOUTHWAITE and N. J. PETCH, *Philos. Mag.* **7** (1962) 45.
145. K. J. KURZYDLOWSKI, *J. Mater. Sci. Lett.* **9** (1990) 788.
146. J. H. GITTUS, in "Modelling Small Deformations of Polycrystals", edited by J. H. Gittus and J. Zarka (Elsevier, London, 1986) p. 149.
147. L. SHI and D. O. NORTHWOOD, *Acta Metall. Mater.* (1992) submitted.
148. P. LIN, PhD dissertation, University of California, Los Angeles (1984).
149. J. P. HIRTH and J. LOTHE, in "Theory of Dislocations" (McGraw-Hill, New York, 1968) p. 510.
150. A. EINSTEIN, *Ann. Physik* **17** (1905) 549.
151. *Idem*, in "Investigations on the Theory of the Brownian Movement" (Dover, New York, 1956) p. 1.
152. C. A. WERT and R. M. THOMSON, in "Physics of Solids", 2nd Edn (McGraw-Hill, New York, 1970) p. 319.
153. M. PEACH and J. S. KOEHLER, *Phys. Rev.* **80** (1950) 436.
154. J. WEERTMAN, *Philos. Mag.* **11** (1965) 1217.
155. F. R. N. NABARRO, *ibid.* **16** (1967) 231.
156. W. D. NIX, R. GASCA-NERI and J. P. HIRTH, *ibid.* **23** (1971) 1339.
157. M. J. TURUNEN and V. K. LINDROOS, *ibid.* **27** (1973) 81.
158. J. H. GITTUS, in "Creep, Viscoelasticity and Creep Fracture in Solids" (Wiley, New York, 1975) p. 113.
159. J. C. M. LI, *Can. J. Phys.* **45** (1967) 493.
160. *Idem*, in "Dislocation Dynamics", edited by A. R. Rosenfield, G. T. Hahn, A. L. Bement Jr and R. I. Jaffee (McGraw-Hill, New York, 1968) p. 87.
161. A. S. KRAUSZ and H. EYRING, in "Deformation Kinetics" (Wiley, New York, 1975) p. 180.
162. U. F. KOCKS, A. S. ARGON and M. F. ASHBY, *Prog. Mater. Sci.* **19** (1975) 1.
163. *Idem, ibid.* **19** (1975) 110.
164. H. J. FROST and M. F. ASHBY, in "Deformation-Mechanism Maps, The Plasticity and Creep of Metals and Ceramics" (Pergamon, Oxford, 1982) p. 1.
165. J-P. POIRIER, in "Creep of Crystals, High-Temperature Deformation Processes in Metals, Ceramics and Minerals" (Cambridge University Press, Cambridge, 1985) p. 49.
166. Y. LIU, J. ZHU and H. ZHOU, *Metall. Trans.* **23A** (1992) 335.

Received 13 January
and accepted 19 March 1993